



Strontium ferrite $\text{SrFeO}_{3-\delta}$ ($2.50 \leq 3-\delta \leq 2.87$) studied by Raman and Mössbauer spectroscopy

O.I. Barkalov^{*}, S.V. Zaitsev, V.D. Sedykh

Ossipyan Institute of Solid State Physics Russian Academy of Sciences, Chernogolovka, Moscow District, 2 Academician Ossipyan str., 142432 Russia

ARTICLE INFO

Communicated by Zhao Liuyan

Keywords:

Strontium ferrite
Browmillerite
Raman spectroscopy
Mössbauer spectroscopy

ABSTRACT

Crystal structure, short range order, lattice dynamics and valence state of polycrystalline single-phase strontium ferrites $\text{SrFeO}_{3-\delta}$ (with $3-\delta = 2.87 \div 2.5$) were studied by Raman and Mössbauer spectroscopy at normal conditions. Valence states of Fe ions and their fractions were determined from Mössbauer spectroscopy and concentrations of oxygen in all phases were estimated. For all studied $\text{SrFeO}_{3-\delta}$ phases only five (or less) bands were observed above 200 cm^{-1} in spite of numerous Raman active phonon modes predicted by a factor group analysis. For the antiferromagnetic Browmillerite phase ($3-\delta = 2.5$), a broad band observed at $\sim 1350\text{--}1400 \text{ cm}^{-1}$, was attributed to the two-magnon scattering. This band was found also for the $\text{SrFeO}_{3-\delta}$ samples with $3-\delta = 2.87 \div 2.725$ which are in paramagnetic state at room temperature. This fact indicates an existence of the unusual magnetic correlations in all $\text{SrFeO}_{3-\delta}$ perovskites.

1. Introduction

Being antiferromagnetic (AFM), $\text{SrFeO}_{3-\delta}$ ferrite recently acquired sufficient deal of interest. Absence of the net magnetization and stray fields make antiferromagnets attractive for applications in magnetic memory devices. Comparing to the ferromagnets they are characterized by ultrafast spin dynamics due to the absence of the macroscopic magnetization [1]. Antiferromagnetic materials are promising for applications such as non-volatile memory and other magnetic devices with multilayer structures [2]. The $\text{SrFeO}_{3-\delta}$ oxide belonging to this family of materials is a compound with an anion-deficient perovskite-type structure, in which Fe cations can have a mixed valence state: Fe^{4+} , Fe^{3+} and the averaged valence state $\text{Fe}^{3.5+}$ [3]. The physical properties of anion-deficient perovskite-type oxides $\text{SrFeO}_{3-\delta}$ are extremely sensitive to variations of oxygen content [3], which is dependent on the synthesis conditions. Thus, variation of “ $3-\delta$ ” parameter changes iron atoms valence state and the $\text{Fe}^{3+}/\text{Fe}^{4+}$ ratio in the compound. The later, in its turn, induces alterations of the crystalline structure, magnetic order, electrical conductivity [4]. Sensitiveness of the material properties to existence and amount of oxygen vacancies opens another application field as oxygen gas gauges and fuel cells materials [5–7]. Despite of the numerous structural data available and assumptions concerning the origin of different $\text{SrFeO}_{3-\delta}$ structural arrangements the interplay of the charge state of Fe atoms, structural ordering of oxygen vacancies and

magnetic structure of materials remains unclear yet. Raman spectroscopy is the promising experimental method to explore the atomic electron configurations and vibrational behavior of the materials [8].

Since first observations, a large number of theoretical and experimental works on Raman scattering by two magnons in antiferromagnets has shown the large effect of magnon-magnon interactions [9]. Recently the magnetic ordering in $\text{SrFeO}_{3-\delta}$ and related compounds was explored thoroughly by two-magnon Raman scattering [10–13].

Up to date the Raman spectroscopy studies of $\text{SrFeO}_{3-\delta}$ were focused on the frequency range below 1000 cm^{-1} since its main phonon modes fall into this interval. The lack of information at higher frequencies motivated our studies and in the present work the $\text{SrFeO}_{3-\delta}$ oxide with $3-\delta = 2.87 \div 2.50$ was investigated by Raman spectroscopy in the wide range of $250\text{--}2000 \text{ cm}^{-1}$. We observed rather prominent two-magnon Raman band at $\sim 1400 \text{ cm}^{-1}$ in addition to the well-known Raman features at low frequencies.

2. Methods

Samples of strontium ferrite $\text{SrFeO}_{3-\delta}$ under investigation with oxygen content $3-\delta$ varying from 2.87 to 2.50 were synthesized in air using sol-gel method. Nitrates $\text{Sr}(\text{NO}_3)_2$ and $\text{Fe}(\text{NO}_3)_3 \cdot 9\text{H}_2\text{O}$ were used in the stoichiometric proportion as initial materials [3]. This preparation method was used as it proved to produce homogeneous samples with

^{*} Corresponding author.

E-mail addresses: barkalov@issp.ac.ru (O.I. Barkalov), szaitsev@issp.ac.ru (S.V. Zaitsev), sedykh@issp.ac.ru (V.D. Sedykh).

<https://doi.org/10.1016/j.ssc.2022.114912>

Received 27 April 2022; Received in revised form 11 July 2022; Accepted 21 July 2022

Available online 8 August 2022

0038-1098/© 2022 Published by Elsevier Ltd.

high degree of crystalline ordering. As-prepared $\text{SrFeO}_{2.80}$ was subjected then either to vacuum annealing (10^{-3} Torr) or to oxygen saturation (1 atm. O_2) at $450\text{ }^\circ\text{C} \div 650\text{ }^\circ\text{C}$ for 4 h in order to get samples with lower and higher oxygen concentration, respectively. Phase composition, crystalline structure and local atomic order of Fe ions were studied by powder X ray diffraction and Mössbauer spectroscopy. The results of these studies and details of the experimental methods were reported elsewhere [3]. One should note that the prepared samples are agglomerates of particles with sizes varying from a few fractions of micrometer to dozens of micrometers as was observed in electron-microscopy studies [3].

Raman spectra were recorded with the Princeton Instruments HRS 500 spectrometer equipped with a liquid nitrogen cooled charge coupled device detector and a grating of 1200 grooves/mm. The samples were irradiated at room temperature with a 532 nm laser line (KLM-532/SLN-100 DPSS, Optronic) with the laser power of about 5 mW at the sample using a back-scattering geometry. A 20x Plan Apo Mitutoyo objective

was used to focus the laser beam to a spot of approximately $3\text{ }\mu\text{m}$ in size and collect the scattered light. Holographic Notch filter (Tydex) was used for laser line discrimination and acquiring Raman spectra higher than 200 cm^{-1} . The spectral resolution in the studied spectral range was $\approx 1\text{ cm}^{-1}$. The Raman spectrometer was calibrated using Ne spectral lines with an uncertainty of $\pm 1\text{ cm}^{-1}$.

The Mössbauer measurements were carried out on polycrystalline samples using a CM 1101 spectrometer operating in the constant acceleration mode using $^{57}\text{Co}(\text{Rh})$ as a radioactive source. The Mössbauer absorption spectra were analyzed by the MossFit 3.1 software package for the spectra decomposition into the partial spectra approximated by a sum of analytical functions. The program algorithms assumed a thin absorber approximation.

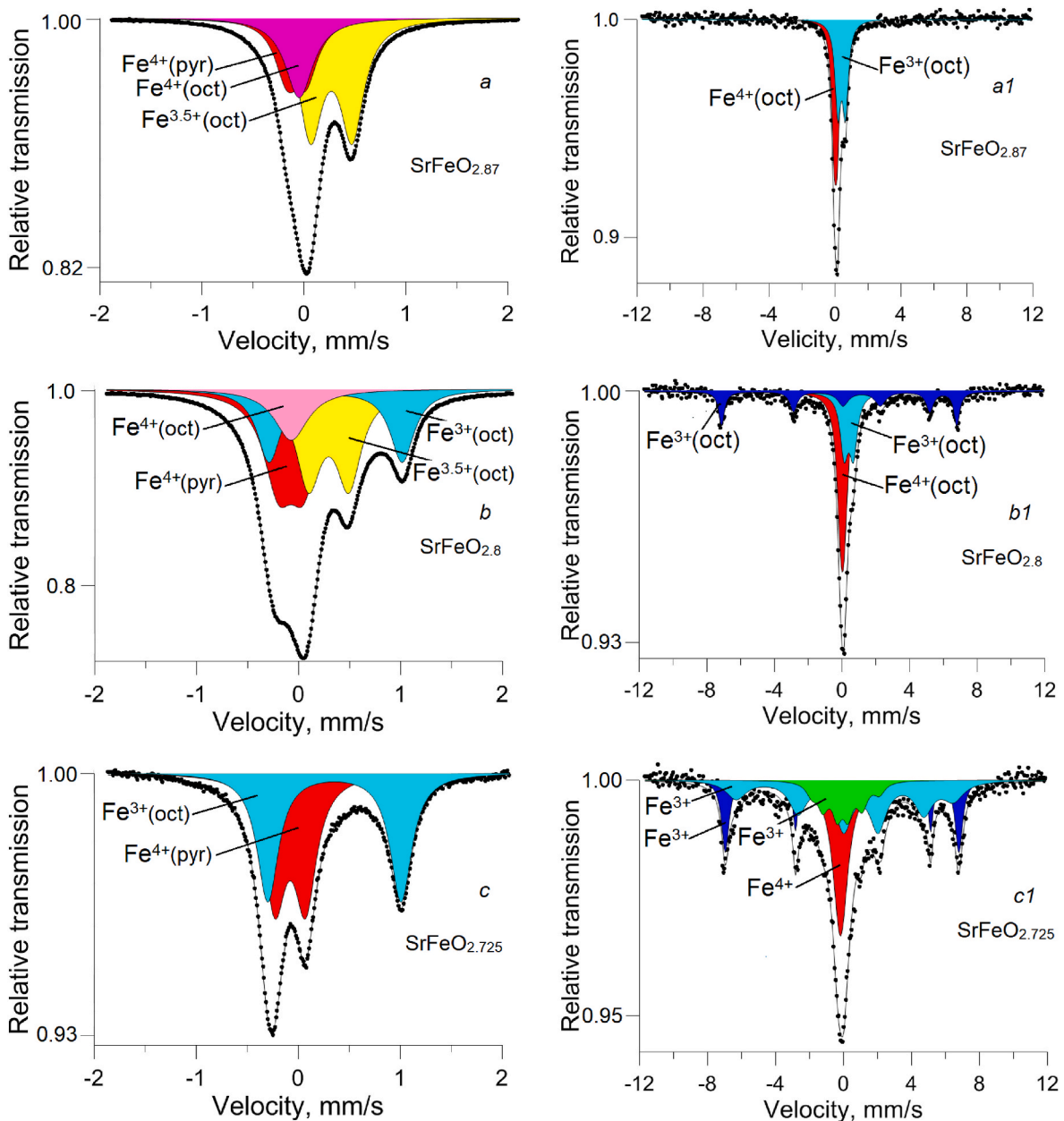


Fig. 1. Mössbauer spectra measured: (a,b,c) at 300 K, (a1,b1,c1) at 90 K, $\text{SrFeO}_{2.87}$, tetragonal phase (sample annealed in oxygen), $\text{SrFeO}_{2.80}$, tetragonal phase (as-prepared sample), $\text{SrFeO}_{2.725}$, orthorhombic phase (sample annealed in vacuum).

3. Results and discussion

3.1. Mössbauer spectroscopy

The detailed Mössbauer spectroscopy study of $\text{SrFeO}_{3-\delta}$ oxide structural features was reported in our previous publication [14]. In the present work the necessary results of [3,14] are given in brief for the sake of convenience to use them for analysis of the Raman spectroscopy data in the next section.

In anion-deficient $\text{SrFeO}_{3-\delta}$ oxide the following single-phase structures are possible depending on oxygen content [3,14]. The cubic SrFeO_3 compound with iron ion in pure tetravalent state is free of oxygen vacancies. The $\text{SrFeO}_{2.875}$ has tetragonal structure at room temperature, in which iron ions are in Fe^{4+} valence state with octahedral ($\text{Fe}^{4+}(\text{oct})$) and pyramidal ($\text{Fe}^{4+}(\text{pyr})$) oxygen environment and in the $\text{Fe}^{3.5+}$ averaged-valence state with octahedral ($\text{Fe}^{3.5+}(\text{oct})$) oxygen environment. The $\text{SrFeO}_{2.75}$ oxide has orthorhombic structure in which the $\text{Fe}^{3.5+}$ ions transform into Fe^{3+} valence state with octahedral ($\text{Fe}^{3+}(\text{oct})$) oxygen environment, Fe^{4+} ions are only in pyramidal ($\text{Fe}^{4+}(\text{pyr})$) oxygen environment. So, the Fe^{4+} ions are present in all these compounds.

The Brownmillerite $\text{SrFe}_{2.5}$ compound has only Fe^{3+} ions, but in two different oxygen environments, octahedral ($\text{Fe}^{3+}(\text{O})$) and tetrahedral ($\text{Fe}^{3+}(\text{T})$) ones. The characteristic Mössbauer spectra measured at 300 and 90 K for single phase $\text{SrFeO}_{3-\delta}$ structures, $\text{SrFeO}_{2.87}$, $\text{SrFeO}_{2.80}$, $\text{SrFeO}_{2.725}$, are presented in Fig. 1. These phases are paramagnetic at room temperature. The Mössbauer spectra measured at 300 K for $\text{SrFe}_{2.62}$ containing the paramagnetic orthorhombic $\text{SrFeO}_{2.725}$ and magnetic Brownmillerite phases in equal proportion and $\text{SrFeO}_{2.5}$ Brownmillerite phase are presented in Fig. 2.

The experimental Mössbauer spectra of $\text{SrFeO}_{3-\delta}$ ($3-\delta = 2.87 \div 2.725$) measured at 300 K and 90 K were decomposed into partial subspectra corresponding to the iron ions in different valence states as shown in Fig. 1. Parameters of the subspectra including the fraction of each subspectra (A) are presented in Table 1. Using the fraction values we calculated the averaged iron ion valence state and then the oxygen content in ferrite ($3-\delta$) given in the first column of Table 1 in brackets. Mössbauer subspectra parameters for two-phase $\text{SrFeO}_{2.62}$ ferrite and single Brownmillerite phase $\text{SrFeO}_{2.5}$ studied at 300 K are given in Table 2.

The low temperature Mössbauer spectra demonstrate increasing of the Néel temperature with decreasing the oxygen content in the $\text{SrFeO}_{3-\delta}$ oxides. Thus, the $\text{SrFeO}_{2.87}$ is still paramagnetic at 90 K while the magnetic contribution in Mössbauer spectrum of $\text{SrFeO}_{2.80}$ appears at 90 K.

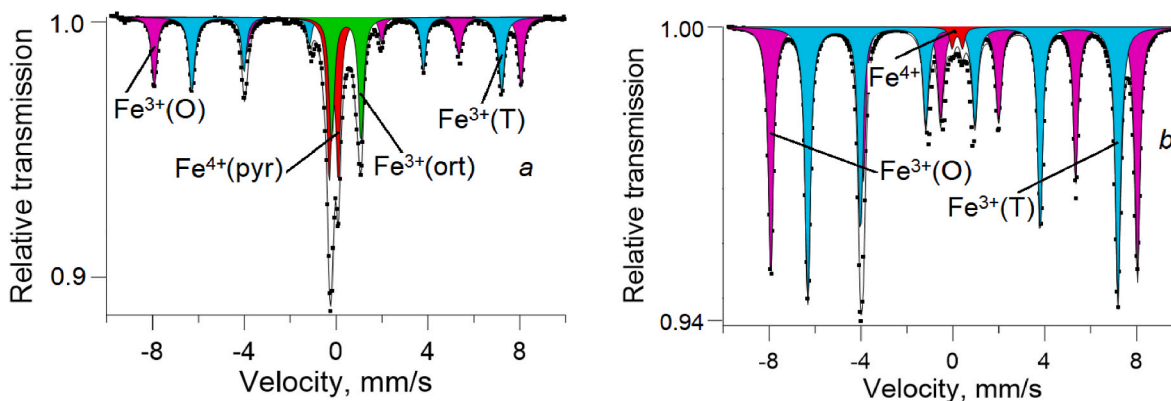


Fig. 2. Mössbauer spectra measured at 300 K (a) of two-phase $\text{SrFeO}_{2.62}$ containing 50% Brownmillerite and 50% orthorhombic phase, (b) $\text{SrFeO}_{2.5}$, Brownmillerite phase. The Octahedral and Tetrahedral environments of Fe^{3+} ion in the Brownmillerite phase are labeled by (O) and (T), respectively.

3.2. Raman spectroscopy

Representative Raman spectra of $\text{SrFeO}_{3-\delta}$ for oxygen content $3-\delta$ varying from 2.87 to 2.5 compounds are shown in Fig. 3. Peak positions of the Raman active modes monitored within the $250\text{--}2000\text{ cm}^{-1}$ interval are plotted as a function of $3-\delta$ parameter in Fig. 4. It should be stressed that in the present work the oxygen contents in all samples were determined from Mössbauer data while in Ref. [12] the “ $3-\delta$ ” values were determined by the thermogravimetry method. Experimental points obtained by this direct method in Ref. [12] fit sufficiently well to the smooth curves formed by the data in the present work. This effect indicates the adequate accuracy of the method applied in the present work for oxygen content determination.

Gradual oxygen release induces the following series of structural phase transitions in the strontium ferrite. For the starting compound SrFeO_3 with high symmetry cubic structure there are no active Raman modes [11,12]. For lower $3-\delta = 2.87$ oxygen concentration a tetragonal structure ($I4/mmm$ space group) is stable. This sample was prepared by annealing of the as-prepared material ($3-\delta = 2.80$) under oxygen atmosphere. Vacuum annealing (10^{-3} Torr) at $450\text{ }^\circ\text{C}$ for 4 h of the as-prepared sample results in formation of the orthorhombic crystal structure with $3-\delta = 2.725$ with the space group $Cmmm$. Vacuum annealing at $650\text{ }^\circ\text{C}$ for 4 h leads to Brownmillerite type compound $\text{SrFeO}_{2.5}$ with orthorhombic space group $Ibm2$. The sample of intermediate composition annealed at $450\text{ }^\circ\text{C}$, $3-\delta = 2.62$, is a two-phase mixture of Brownmillerite and orthorhombic phase, as demonstrated by imposing red and gray spectra in Fig. 5 and was confirmed by the Mössbauer and X-ray diffraction data in Ref. [14]. Black and gray spectra monitored at the different points of Brownmillerite $\text{SrFeO}_{2.5}$ sample (Fig. 5) contain similar peak sets with practically the same peak positions while the peaks at the gray spectrum are significantly broadened in contrast to those at the black spectrum.

As demonstrated in the review published by M. Kitajima [15] the Raman peak broadening is caused by a substantial increase of the structural defects fraction in the materials and, hence, decreasing of the grain size down to a nanometer range. The defects were induced in graphite, Si [15], GaAs [16] by high energy ions irradiation or by vacuum annealing of TiO_2 [17] and by varying the grain size in the nanocrystalline CeO_2 thin films [18]. We assume the similar reasons of the effect observed for the Brownmillerite $\text{SrFeO}_{2.5}$ phase. Thereby, the degree of the lattice perfection of $\text{SrFeO}_{2.5}$ sample varies from point to point on a micron length scale.

Formation of the Brownmillerite phase in the sample manifests itself by essential complication and modification of the observed Raman spectra (see Fig. 3). Low-frequency peak at $\sim 300\text{ cm}^{-1}$ is split. Another mode at $\sim 400\text{ cm}^{-1}$ disappeared at all, three peaks in the $600 \div 700\text{ cm}^{-1}$ range are now well resolved. Interestingly, that in the Brownmillerite

Table 1

Mössbauer parameters of the subspectra measured at 300 K and 90 K for the as-prepared SrFeO_{3-δ} sample (AP), and also for the samples annealed in vacuum (AV) and oxygen (AO). IS is the isomer shift (with respect to bcc Fe at 300 K); Δ is the quadrupole splitting; Γ is the Mössbauer line width; H_n is the effective magnetic field on a ⁵⁷Fe nucleus for various iron ion sites in the lattice; A is the portion of each subspectrum.

Sample (3-δ)	Valence of iron ion	300 K				90 K				
		IS, mm/s	Δ, mm/s	Γ, mm/s	A, %	IS, mm/s	Δ, mm/s	Γ, mm/s	H _n , kOe	A%
AO (2.87)	4+	-0.05		0.29	14					
	4+	-0.08	0.19	0.30	33	-0.04	0.19	0.37		51
	3.5+	0.27	0.41	0.27	53	0.40	0.46	0.42		49
AP (2.80)	4+	-0.06		0.31	15					
	4+	-0.09	0.22	0.29	30	-0.04	0.27	0.49		46
	3.5+	0.27	0.40	0.28	41	0.40	0.59	0.69		39
	3+	0.38	0.69	0.36	4					
	3+	0.36	1.30	0.34	10	0.49	1.28	0.5	433	15
AV (2.725)	4+	-0.08	0.29	0.29	46	-0.08	0.16			49
	3+	0.32	0.28	0.32	5	0.25	0.58		243	13
	3+	0.41	0.70	0.32	4					
	3+	0.35	1.31	0.27	45	0.54	-1.22		434	38

Table 2

Parameters of the Mössbauer subspectra at 300 K of the SrFeO_{3-δ} annealed in vacuum at 450 °C (450AV) and 650 °C (650AV). **Ortho** is the orthorhombic phase, **Brm** is the brownmillerite phase; Sx-1 and Sx-2 are magnetic sextets for Fe³⁺(O) and Fe³⁺(T), respectively, D-1 and D-2 are paramagnetic doublets for Fe⁴⁺(pyr) and Fe³⁺(ort), respectively; IS is the isomer shift (with respect to bcc Fe at 300 K); Δ is the quadrupole splitting; H_n is the effective magnetic field on a ⁵⁷Fe nucleus for Sx-1 and Sx-2; A is the contribution of the given subspectrum.

Annealing	Phase	Subspectrum	IS, mm/s	Δ, mm/s	H _n , kOe	A, %	3-δ
450AV	Brm	Sx-1	0.38 (1)	0.66 (1)	496 (1)	23	2.62
		Sx-2	0.17 (1)	-0.56 (1)	419 (1)	26	
	Ortho	D-1	-0.09 (1)	0.39 (1)		24	
		D-2	0.42 (1)	1.28 (1)		27	
650AV	Brm	Sx-1	0.38 (1)	0.67 (1)	496 (1)	44	2.5
		Sx-2	0.17 (1)	-0.57 (1)	420 (1)	50	
	Ortho	D-1	0.23 (5)	0.36 (5)		2	
		D-2	0.24 (5)	1.17 (5)		4	

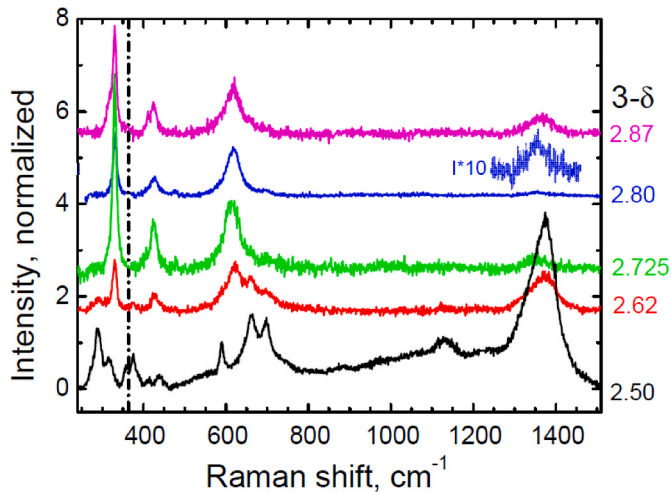


Fig. 3. Representative Raman spectra of SrFeO_{3-δ} samples with various oxygen contents. The spectra were normalized by the intensity of the peak at ~600 cm⁻¹ of SrFeO_{2.5}. The oxygen content (3-δ) of the sample is given at the right side of the plot. The vertical dash-and-dot line denotes the position of the parasitic laser line at ~364 cm⁻¹. Smooth and featureless background caused by the sample luminescence was subtracted manually from the spectra.

structure we observed a very weak Raman band at ~1130 cm⁻¹ tentatively attributed to the two-phonon Raman scattering caused by a strong coupling with spin subsystem in the AFM phase [20].

Broad feature in 1350 ÷ 1400 cm⁻¹ frequency range is observed for all SrFeO_{3-δ} compositions (been extremely weak for 3-δ = 2.80 tetragonal phase it is shown in a large scale in Fig. 3 above the main spectrum). The tetragonal and orthorhombic samples (3-δ = 2.87, 2.80 and 3-δ =

2.725, respectively) at room temperature are in the paramagnetic state, nevertheless, the two-magnon peaks are detected. We assume that the fragments of antiferromagnetic chains of few nanometers length still persist in their magnetic lattices. The extremely low amplitude of the two-magnon peak for tetragonal sample with 3-δ = 2.80 is, possibly, due to the high degree of the magnetic disorder for this very composition. The iron cations in it are in 3+, averaged-valence 3.5+ and 4+ oxidation states. For Brownmillerite phase, which is AFM at room temperature, the relative intensity of the two-magnon peak is extremely high. The broad peak at ~1370 cm⁻¹ was attributed in Ref. [13] to the two-magnon scattering in this AFM compound with the highest among others SrFeO_{3-δ} ferrites Néel temperature T_N ~ 673 K [21]. The two-magnon scattering in the AFM crystal involves excitation of two magnons, with one magnon on each sublattice [10,11]. It should be stressed that the two-magnon excitations well above Néel temperature were observed also for micro- and nanoparticles of Fe₂O₃ synthesized by sol-gel method (T_N = 450 K) [22]. Such a magnetic excitation above T_N with rather complicated origin is called paramagnon and represents the object of intensive studies during last years [23].

Full and reliable assignment of the phonon modes of SrFeO_{3-δ} phases has not been accomplished yet due to the following reason. Even for the high symmetrical tetragonal compound SrFeO_{2.87} a factor group analysis at Γ point reveals 31 active modes [12,24,25] while only four peaks (three phonon peaks and one two-magnon peak) are resolved in the spectrum, presumably, due to low intensity of the modes, see Fig. 3. As reported in Refs. [12,25] decreasing temperature below 70 K (charge ordering phase transition) resulted in prominent modification of the observed spectra.

Numerous new peaks were observed below this temperature. To proceed with the assignment one needs to perform *ab initio* calculations of modes frequencies and their relative intensities, similar to those reported by A. Piovano et al. for CaFeO_{2.5} [19]. Regrettably, a direct

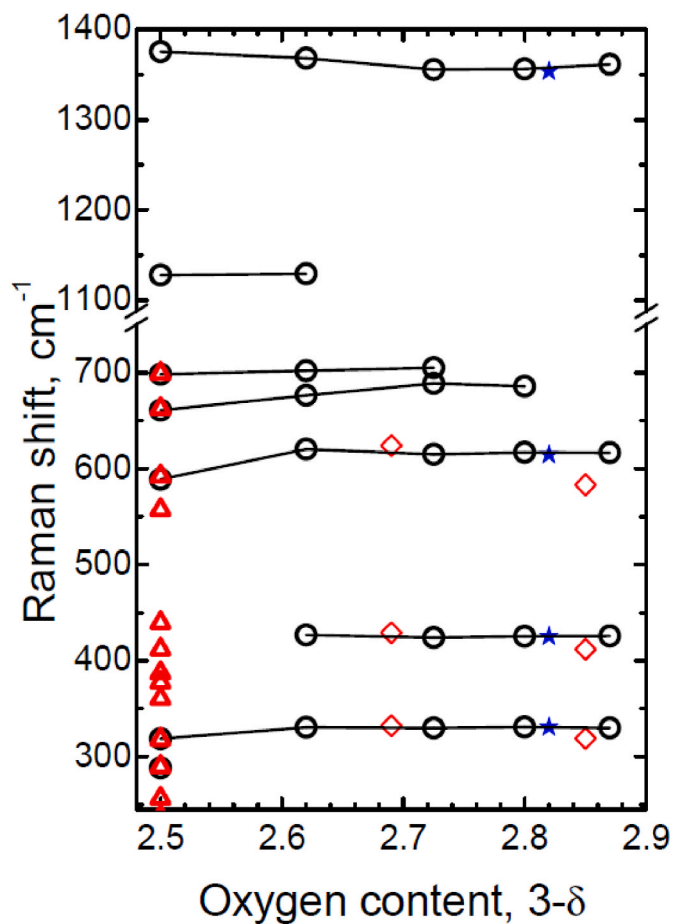


Fig. 4. Frequencies of the Raman active modes of $\text{SrFeO}_{3-\delta}$ plotted as a function of the oxygen content in the sample ($3-\delta$). The open black circles represent the results of the present work, red diamonds stand for the data reported in Ref. [12] and blue stars show the results of [13]. Exact oxygen content in the sample studied in Ref. [13] was not determined, however, the crystal structure of the sample was tetragonal, so, formally we assigned it to $3-\delta = 2.82$. The red triangles denote the peak positions of the $\text{SrFeO}_{2.5}$ reported in Ref. [19]. The lines drawn through the data points are the guides for the eye. (For interpretation of the references to colour in this figure legend, the reader is referred to the Web version of this article.)

comparison of phonon modes with the results of Ref. [19] is not possible because of different crystal structures of $\text{CaFeO}_{2.5}$ and $\text{SrFeO}_{2.5}$ compounds.

4. Conclusions

Summarizing the results obtained we come to the following conclusions. Our spectroscopic data justify that the oxygen content in $\text{SrFeO}_{3-\delta}$ prepared by sol-gel method and subsequently annealed in vacuum or in oxygen can be estimated by using the iron ions oxidation numbers determined from the Mössbauer spectra of the compounds. The uncertainties of this method are comparable with those of the direct method based on thermogravimetric scans reported in Ref. [12].

A broad Raman band observed in all studied samples in the high frequency region at $\sim 1375 \text{ cm}^{-1}$ is attributed to the two-magnon scattering. Observation of this band not only for the antiferromagnetic Brownmillerite phase ($3-\delta = 2.5$) but also for all other $\text{SrFeO}_{3-\delta}$ phases, paramagnetic at room temperature, indicates a rather strong magnetic correlations in all studied $\text{SrFeO}_{3-\delta}$ perovskites. Tentatively these magnetic correlations are attributed to the paramagnons [23] but exact modes assignment requires detailed Raman studies in a wide temperature range. Measurements in the low frequency range (below 1000

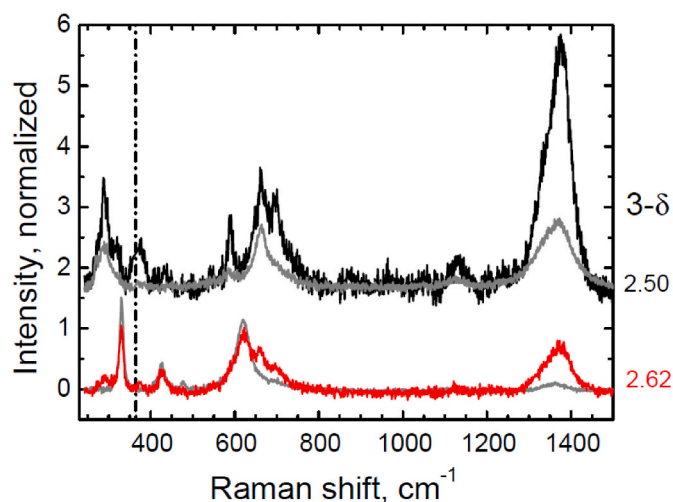


Fig. 5. Raman spectra of $\text{SrFeO}_{3-\delta}$ samples with the oxygen contents of $3-\delta = 2.50, 2.62$. Black and red lines represent the spectra shown in Fig. 3 while gray lines show the spectra measured at another points of the samples. The spectra were normalized by the intensity of the peak at $\sim 600 \text{ cm}^{-1}$ of $\text{SrFeO}_{2.5}$. The oxygen content ($3-\delta$) of the sample is given at the right side of the plot. The vertical dash-and-dot line denotes the position of the parasitic laser line at $\sim 364 \text{ cm}^{-1}$. Smooth and featureless background caused by the sample luminescence was subtracted manually from the spectra. (For interpretation of the references to colour in this figure legend, the reader is referred to the Web version of this article.)

cm^{-1}) revealed only few Raman phonon modes in contradiction to numerous active modes predicted by a factor group analysis. This discrepancy requires additional investigations at low temperatures.

Credit author statement

O.I. Barkalov: Investigation, Writing – review & editing. S.V. Zaitsev: Investigation, Writing – review & editing. V.D. Sedykh: Conceptualization, Validation, Writing – review & editing.

Declaration of competing interest

The authors declare that they have no known competing financial interests or personal relationships that could have appeared to influence the work reported in this paper.

Data availability

No data was used for the research described in the article.

Acknowledgments

The authors wish to acknowledge using the micro-Raman optical system of the Multiple-access Center in the Osipyan Institute of Solid State Physics RAS (Chernogolovka) for the data acquisition. This work was carried out within the framework of the State task of the Osipyan Institute of Solid State Physics Russian Academy of Sciences.

References

- [1] A. Kirilyuk, A.V. Kimel, T. Rasing, Ultrafast optical manipulation of magnetic order, *Rev. Mod. Phys.* vol. 82 (2010) 2731–2784.
- [2] K. Takano, R.H. Kodama, A.E. Berkowitz, W. Cao, G. Thomas, Role of interfacial uncompensated antiferromagnetic spins in unidirectional anisotropy in $\text{Ni}_81\text{Fe}_{19}/\text{CoO}$ bilayers (invited), *J. Appl. Phys.* 83 (1998) 6888–6892.
- [3] V.D. Sedykh, O.G. Rybchenko, A.N. Nekrasov, I.E. Koneva, V.I. Kulakov, Effect of the oxygen content on the local environment of Fe atoms in anion-deficient $\text{SrFeO}_{3-\delta}$, *Phys. Solid State* 61 (2019) 1099–1106.

- [4] A.A. Bush, V.A. Sarin, D.G. Georgiev, V.M. Cherepanov, Synthesis, X-ray and neutron diffraction and Mössbauer studies of SrFeO_x crystals, *Crystallogr. Rep.* 45 (2000) 734–738.
- [5] M.J. Akhtar, R.T.A. Khan, Structural studies of SrFeO₃ and SrFe_{0.5}Nb_{0.5}O₃ by employing XRD and XANES spectroscopic techniques, *Mater. Char.* 62 (2011) 1016–1020.
- [6] C. Srilakshmi, R. Saraf, C. Shivakumara, Effective degradation of aqueous nitrobenzene using the SrFeO_{3-δ} photocatalyst under UV illumination and its kinetics and mechanistic studies, *Ind. Eng. Chem. Res.* 54 (2015) 7800–7810.
- [7] M.H. Ghaffari, O. Huang, Tana K, Band gap measurement of SrFeO_{3-δ} by ultraviolet photoelectron spectroscopy and photovoltage method, *CrystEngComm* 14 (2012) 7487–7492.
- [8] M. Cardona (Ed.), *Light Scattering in Solids I*, Springer-Verlag Berlin Heidelberg, 1983. <https://www.springer.com/gp/book/9783540119135>.
- [9] G.B. Wright (Ed.), *Light Scattering Spectra of Solids*, Springer-Verlag Berlin Heidelberg, 1969. <https://www.springer.com/gp/book/9783642873591>.
- [10] J. Andreasson, J. Holmlund, C.S. Knee, M. Käll, L. Börjesson, et al., Franck-Condon higher order lattice excitations in the LaFe_{1-x}Cr_xO₃ (x=0, 0.1, 0.5, 0.9, 1.0) perovskites due to Fe-Cr charge transfer effects, *Phys. Rev. B* 75 (2007) 104302.
- [11] S. Manzoor, S. Husain, V. Raghavendra Reddy, Epitaxial LaFeO₃ and LaFe_{0.75}Zn_{0.25}O₃ thin films on SrTiO₃ (STO) (100) substrate: structural studies and high energy magnon excitations, *Appl. Phys. Lett.* 113 (2018), 072901.
- [12] P. Adler, A. Lebon, V. Damljanović, C. Ulrich, C. Bernhard, V. Boris A, A. Maljuk, C. T. Lin, B. Keimer, Magnetoresistance effects in SrFeO₃: dependence on phase composition and relation to magnetic and charge order, *Phys. Rev. B* 73 (2006), 094451.
- [13] A.S. Anokhin, A.G. Razumnaya, V.I. Torgashev, V.G. Trotsenko, I. Zyuziyu Yu, A. A. Bush, V Ya Shkuratov, B.P. Gorshunov, E.S. Zhukova, L.S. Kadyrov, G. A. Komandin, Dynamic spectral response of solid solutions of the bismuth-strontium ferrite Bi_{1-x}Sr_xFeO_{3-δ} in the frequency range 0.3–200 THz, *Phys. Solid State* 55 (2013) 1417–1430.
- [14] V.D. Sedykh, O.G. Rybchenko, E.V. Suvorov, A.I. Ivanov, V.I. Kulakov, Oxygen vacancies and valence states of iron in SrFeO_{3-δ} compounds, *Phys. Solid State* 62 (2020) 1916–1923.
- [15] M. Kitajima, Defects in crystals studied by Raman scattering, *Crit. Rev. Solid State Mater. Sci.* 22 (1997) 275–349.
- [16] K.K. Tiong, P.M. Amirtharaj, F.H. Pollak, D.E. Aspnes, Effects of As⁺ ion implantation on the Raman spectra of GaAs: “Spatial correlation” interpretation, *Appl. Phys. Lett.* 44 (1984) 122–124.
- [17] R.J. Betsch, H.L. Park, W.B. White, Raman spectra of stoichiometric and defect rutile Mat, *Res. Bull.* 26 (1991) 613–622.
- [18] I. Kosacki, T. Suzuki, H.U. Anderson, P. Colomban, Raman Scattering and lattice defects in nanocrystalline CeO₂ thin films, *Solid State Ion.* 149 (2002) 99–105.
- [19] A. Piovano, M. Ceretti, M.R. Johnson, G. Agostini, W. Paulus, C. Lamberti, Anisotropy in the Raman scattering of a CaFeO_{2.5} single crystal and its link with oxygen ordering in Brownmillerite frameworks, *J. Phys. Condens. Matter* 27 (2015), 225403.
- [20] M.O. Ramirez, M. Krishnamurthi, S. Denev, A. Kumar, et al., Two-phonon coupling to the antiferromagnetic phase transition in multiferroic BiFeO₃, *Appl. Phys. Lett.* 92 (2008), 022511.
- [21] M. Schmidt, S.J. Campbell, Crystal and magnetic structures of Sr₂Fe₂O₅ at elevated temperature, *J. Solid State Chem.* 156 (2001) 292–304.
- [22] J. López-Sánchez, A. Serrano, A. Del Campo, M. Abuíñ, O. Rodríguez de la Fuente, N. Carmona, Sol-gel synthesis and micro-Raman characterization of ε-Fe₂O₃ micro- and nanoparticles, *Chem. Mater.* 28 (2016) 511–518.
- [23] O.P. Sushkov, Paramagnons the long and the short of it, *Nat. Phys.* 10 (2014) 339–340.
- [24] J.P. Hodges, S. Short, J.D. Jorgensen, Evolution of oxygen-vacancy ordered crystal structures in the perovskite series Sr_nFe_nO_{3n-1} (n = 2, 4, 8, and ∞), and the relationship to electronic and magnetic properties, *J. Solid State Chem.* 151 (2000) 190–209.
- [25] V. Damljanović, Raman Scattering, Magnetization and Magnetotransport Study of SrFeO_{3-δ}, Sr₃Fe₂O_{7-δ} and CaFeO₃, PhD Thesis Stuttgart, 2008.